A New Radar Data Post-Processing Quality Control Workflow for the DWD Weather Radar Network

Manuel Werner

Deutscher Wetterdienst, Frankfurter Str. 135, 63067 Offenbach am Main, Germany

(Dated: 21 July 2014)

1. Introduction

The operational use of weather radar data essentially relies on an efficient data quality control. The task is always to separate undesired echoes from meteorological signals by appropriate filtering techniques. These are already part of the signal processing or are later applied to moment data given for each resolution volume. The latter case is frequently denoted as post-processing quality control. The effect of a filter is that either the data is modified or eliminated at locations detected as (partly) spurious. Usually, the performance of a filter will not be perfect in the sense that it sometimes erases a small amount of meteorological signals on the one hand, or misses spurious data, on the other hand. Both represent undesirable scenarios for a national weather service, who is obligated to distribute meteorological end products to authorities like, e.g., air traffic control with legal certainty. Hence, the selection, application, and tuning of filters requires great care. The setup of filters which suits best also depends on the sometimes opposing quality standards of a subsequent application the data will enter.

In association with the upgrade of DWD's radar network to dual-polarisation technique, a new quality control workflow has been developed and installed to better meet the requirements mentioned above. A new post-processing component is now available using dual-polarisation measurements for the quality control of classical reflectivity and radial velocity data, as well as the new polarimetric data itself. As a new feature, corrected versions of horizontal reflectivity, differential reflectivity, horizontal radial velocity, differential phase, and specific differential phase are generated. This represents an extension of the former strategy at DWD, relying on quality flag products (Hassler et al. (2006); Helmert et al. (2008, 2012); Hengstebeck et al. (2010)). For the first time at DWD, the quality control now also comprises an algorithm for propagation path attenuation. Additionally, in the radial velocity, errors caused by the dual-PRF unfolding procedure are revised. Another important property is the coupling of the post-processing algorithms with the data processing at the radar site. For instance, clutter correction based on dual-polarisation measurements (PHIDP, RHOHV, etc.) and clutter information provided by the signal processor Doppler filter are consolidated (cf. Werner and Steinert (2012)). Moreover, information about the current status of the radar system is collected at the radar site by a separate monitoring tool (see Frech (2013)), written to an xml-file, and automatically sent to the post-processing system operated in DWD's central office. This includes, among others, transmitter status, ZDR offsets, current precipitation rate at the radar site, and radome temperature. The new algorithms are realised within a `C++` software framework called POLARA (POLArimetric Radar Algorithms, cf. Rathmann and Mott (2012)), which also hosts the recently developed hydrometeor classification scheme (Steinert (2014)), a method for quantitative precipitation estimation using polarimetry, the mesocyclone detection algorithm (Hengstebeck et al. (2011)), and various techniques for creating radar composites.

The intention of this paper is to give a thorough presentation of the updated radar data quality control workflow at DWD and to introduce the post-processing algorithm suite, including the techniques based on dual-polarisation measurements (Section 2). The results for an example case from the DWD coast radar Rostock are also presented in Section 2. A brief overview on the current and envisaged future usage of data quality control in DWD's radar data processing chain is given in Section 3.

2. New quality control workflow at DWD

Radar data quality control at DWD is performed in two main stages, cf. Figure 1. The first stage is realised in the signal processor. The post-processing quality control tool run in the central office represents the second stage. On each radar computer, hosting the signal processor software, an additional set of radar monitoring tools is operated, which also generates useful input for the post-processing quality control. In this section, it is briefly explained how radar data is acquired. Afterwards, the quality control workflow and the interplay of the two stages and the radar monitoring tool is presented in detail, followed by the presentation of a representative example case from DWD's radar Rostock.

2.1. Radar data acquisition

The DWD radar network consists of 17 radar devices operating with a common scan strategy, which is repeated every five minutes. Each scan cycle starts with a terrain-following low-elevation "precipitation scan" (PRF 600 Hz, max. range 150 km, 250 m range resolution) followed by a "volume scan" with 10 elevations at fixed elevation angles $5.5°$, $4.5°$, $3.5°$, $2.5°$, $1.5°$, $0.5°$, $8.0°$, $12.0°$, $17°$, $25.0°$ (predominantly dual PRF 600/800 Hz, max. range 180 km, 1000 m range resolution). This pattern

Figure 1: Radar data quality control workflow at DWD.

is complemented by a 90° "bird bath" scan performed afterwards, used for radar monitoring and calibration, cf. Frech (2013). The measurements are grouped in data sweeps, each gathered during one full antenna revolution at the respective elevation angle.

2.2. Quality control stage 1: Radar signal processing at the radar site

The first quality control level is represented by the signal processor filters. Here I-Q data based *Doppler* and *Second Trip filtering* can be applied. Moreover, a set of thresholds for *Noise*, *Signal Quality Index*, *Signal Power*, *Clutter Power*, *Co-polar Correlation Coefficient*, and *Speckle filtering* are used to eliminate undesired echoes. After this step, both corrected and uncorrected radar moments are available. In the following, uncorrected moments are denoted with a letter "*U*" at the beginning. For example, we write *UZh* for the uncorrected horizontal reflectivity and just *Zh* for the version corrected by the signal processor filters.

2.3. Quality control stage 2: Post-processing in the central office

The corrected and uncorrected moments are then sent to the central office in Offenbach am Main and enter the second stage of quality control in the post-processing tool. The following data are used: horizontal reflectivity *Zh, UZh*, horizontal radial velocity *Vh, UVh*, differential reflectivity *ZDR, UZDR*, differential phase *UPHIDP*, co-polar correlation coefficient *URHOHV*, horizontal signal-to-noise ratio *SNRh*, horizontal signal quality index *SQIh*, horizontal quantitative Doppler filter clutter correction *CCORh*, and the matrix *CMAP* of flags encoding which signal processor thresholds have been exceeded.

Using these quantities, there are two main goals to achieve. The first goal is to generate respective quality flag products, named *QZh* and *QVh*, for each individual sweep of horizontal reflectivity *Zh* and horizontal radial velocity *Vh* from the precipitation and volume scans. The quality flag products encode for each individual range bin (pixel) a set of quality bits, where each bit refers to one quality relevant phenomenon. This includes

- *signal processor overflow:* the signal processor has filtered out the pixel (e.g., *UZh* contains valid data, *Zh* does not),
- *positive spoke artifacts:* caused, e.g., by WLAN, sun encounter,
- *positive ring artifacts:* caused, e.g., by ships (corner reflectors, side lobe effect),
- *negative spoke artifacts:* caused, e.g., by (partial) beam blockage, or deliberate sector blanking
- *negative ring artifacts:* ring shaped areas without echo, sometimes caused by radar hardware problems
- *stationary clutter:* clutter from immobile objects, buildings, mountains, etc. (radial velocity close to 0 m/s)
- *variable clutter:* birds, insects, airplanes, chaff, etc.,
- *propagation path attenuation*,

- *second trip*,
- *bright band*,
- *radial velocity aliasing*,
- *Doppler filter correction valid:* Doppler filter has legally worked,
- *Doppler filter correction false:* Doppler filter has significantly decreased a meteorological signal close to 0 m/s radial velocity.

Moreover, radar data errors affecting the whole sweep, e.g., corrupt datasets due to a possible temporary technical radar problem are marked in the quality flag products:

- *radar hardware:* a radar hardware problem has occurred,
- *radar maintenance:* radar is under maintenance,
- *radome attenuation:* the radome is wet,
- *corrupt image:* the whole data sweep is corrupt (e.g., radar hardware problem, multiple broad spoke artifacts).

Subsequent meteorological schemes are then equipped with the pre-filtered reflectivity *Zh* and/or radial velocity data *Vh* and the corresponding quality flag products. Each user may individually decide how to proceed in case a quality relevant event in a range bin or the whole sweep has occurred. However, no quantitative corrections can be performed on the basis of the quality flag products. For example, there is no information about the *amount* of attenuation encoded.

Therefore, the second goal is to additionally provide corrected sweeps for horizontal reflectivity (*ZhCorr*) and horizontal radial velocity (*VhCorr*), as well as quality corrected versions of differential reflectivity (*ZDRCorr*), differential phase (*PHIDPCorr*), and specific differential phase (*KDPCorr*). For those range gates, where no valid data value is available, because of any kind of filtering, a so-called *no echo* escape value is encoded. This means, we assume there are no meteorologically relevant scatterers in the pulse volume. For situations, in which the latter can not be decided, a different escape value, called *no data*, is set. This happens, for instance, in the area of blanked sectors, where the transmitter is switched off. Here, no valid data values are received (usually just noise), and the true weather situation is unknown.

An illustration of the whole post-processing workflow in a simplified form is given in Figure 2. The building blocks of the procedure are introduced in the following.

Step 1: *Evaluation of Radar Status*
The first step is the evaluation of the radar status information provided by the radar monitoring tool, which automatically delivers an xml-file for every five minute scan cycle (see Figure 1). For instance, it contains information about *ifd burst power, ifd burst frequency*, and *transmitter forward power status*. If one of these is suspicious, the *radar hardware* flag in the quality products *QZh*, and *QVh* is set. Moreover, the status files encode a five minute precipitation sum based on laser disdrometer information gathered at the radar site. In case a certain threshold is exceeded, the radome is assumed wet and the *radome attenuation* flag is activated in *QZh* and *QVh*. So far, no quantitative correction is performed in this respect. The radar status information also includes *ZDR* offsets. These will be regarded in **Step 5**.

Step 2: *Application of Thresholds*
The main data quality control then starts from the uncorrected reflectivity *UZh*. Initially, it is checked if thresholds for *Signal-To-Noise Ratio*, *Signal Quality Index*, *Doppler Filter Clutter Correction*, and *Co-polar Correlation* are exceeded. The thresholds can either be manually configured, or the same thresholds as used in the signal processor are applied. The latter is realised by looking at the *CMAP* field, which encodes for each range bin which filter thresholds had been exceeded in the signal processor. The outcome of this module then is a corrected version of *UZh*, called *ZhCorr*. *ZhCorr* will be further revised in the upcoming steps.

Step 3: *Single-Polarisation Algorithms*
This step is composed of a set of algorithms based on the corrected reflectivity *ZhCorr*, produced in the previous step, and on the radial velocity *Vh*, provided by the signal processor. Here, basically the methods described in Hengstebeck et al. (2010) are adopted, including detection of spoke and ring artifacts, corrupt image and second trip detection, as well as clutter blacklisting. However, these methods are now complemented by a scheme to correct for errors in the dual-PRF unfolding procedure. In case spoke or ring pixels, clutter blacklisted or second trip pixels are detected, these are removed from *ZhCorr*, and *Vh*. The *corrupt image* detection is based on a matching of the reflectivity sweep data to certain unnatural statistical patterns. If a sweep, as a whole, is thereby considered corrupt, all pixels are removed from *ZhCorr*. An updated *ZhCorr* and a corrected version of *Vh*, named *VhCorr*, are available after this block of algorithms. The detected issues (except dual-PRF unfolding error corrections) are also marked in the respective flag products *QZh*, and *QVh*.

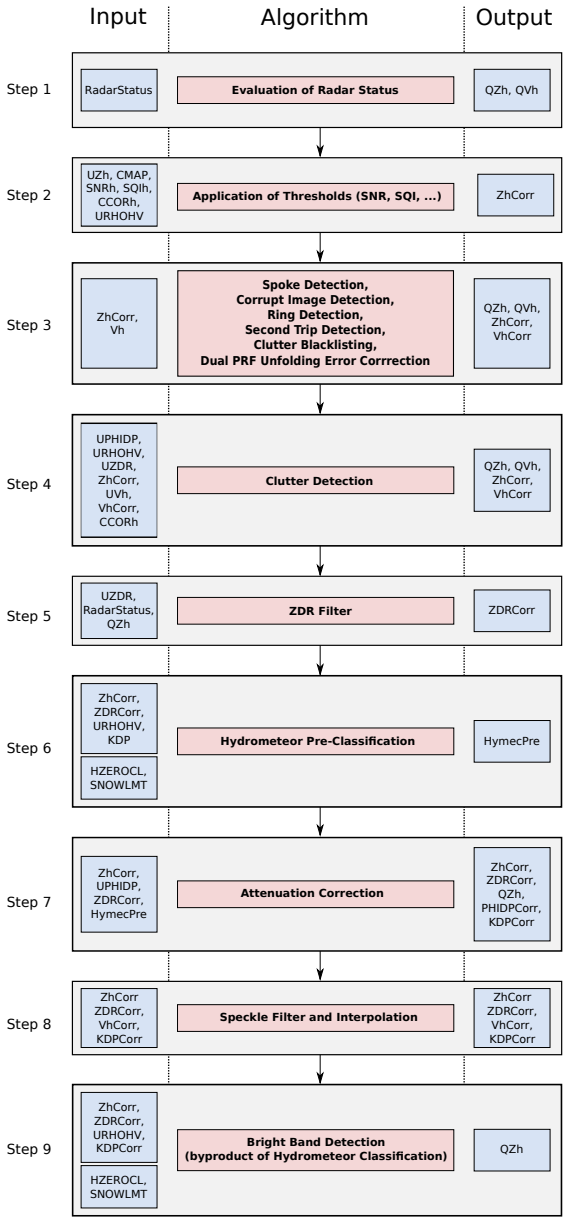

Figure 2: Post-processing quality control workflow.

Step 4: *Clutter Detection*

The clutter detection method is performed range gate by range gate in three steps and essentially relies on the horizontal reflectivity *ZhCorr* (recall **Step 1–3**), uncorrected differential reflectivity *UZDR*, uncorrected differential phase *UPHIDP*, uncorrected co-polar correlation *URHOHV*, see also Werner and Steinert (2012). The detected clutter is marked in the quality products *QZh*, *QVh*, and is, under the conditions described below, also eliminated from *ZhCorr*, and *VhCorr*. The first step consist in a fuzzy logic classifier based on *ZhCorr*, *UZDR*, and *URHOHV* similar to Schuur et al. (2003). The second step combines the outcome of this procedure with information extracted from a *UPHIDP* texture parameter. After this, each range bin is basically assigned to one of the classes *stationary clutter*, *variable clutter*, or *meteorological*. The final stage of this scheme consolidates this result with the potential clutter correction by the signal processor Doppler filter. The following features are realised:

a) In case Doppler filter correction exceeds a (configurable) threshold, then the respective range gate is eliminated in *ZhCorr* and *VhCorr*.

b) In case a significant Doppler correction (e.g., $>$ 3dB) occurs at a range gate classified as meteorological, but where the radial velocity is almost 0 m/s, the *Doppler filter correction false* bit is activated in *QZh*, and *QVh*, no Doppler correction is applied in *ZhCorr*, and the data value in *VhCorr* is taken from *UVh* (*UVh* contains no Doppler correction). Recall that *ZhCorr* originates from *UZh*, and therefore, up to **Step 4**, contained no Doppler filter clutter correction.

c) In the opposite case that the *Doppler filter correction false* bit is not activated, the Doppler filter correction is applied to *ZhCorr*. The value of *VhCorr*, as it originates from *Vh*, is already Doppler corrected, and nothing has to be done here.

d) If the range gate was classified as stationary clutter (radial velocity close to 0 m/s) by the two initial steps, and it was not

eliminated in a), then,

- if the Doppler filter correction is significant (e.g. $>$ 3dB), the quality flag *Doppler filter correction valid* is set in *QZh* and *QVh*. The data value in *ZhCorr* and *VhCorr* can then be kept. This means we assume that the Doppler filter has already suppressed all clutter in this pulse volume. However, in the quality flag products, we leave the stationary clutter bit active, so that the subsequent user is equipped with the full information and may individually decide how to proceed.
- if the Doppler filter correction is less significant (e.g. $\leq$ 3dB), the data values in *ZhCorr* and *VhCorr* are filtered out.

Step 5: *ZDR Filter*
The ZDR filter module takes *UZDR* as input and rigorously eliminates all clutter range gates as well as positive spoke and positive ring pixels based on the respective flags in *QZh*. The result is written to *ZDRCorr*. For the remaining pixels, a reassessment of the ZDR offset is performed as follows. The *Radar Status* xml-file (cf. **Step 1**) contains the fixed ZDR *system offset* already incorporated into *UZDR* by the signal processor. The *Radar Monitoring* uses a 90° bird bath scan with pulse widths 0.4μs and 0.8μs (pulse widths used in the operational scan at DWD) to estimate the current true ZDR offsets. These are as well provided in the *Radar Status* file. The ZDR filter module then subtracts out the system offset and applies the measured true offset for the respective pulse width.

Steps 6 and 7: *Hydrometeor Pre-Classification and Attenuation Correction*
The next goal is to correct horizontal reflectivity and differential reflectivity for attenuation. The corrections are applied to *ZhCorr* and *ZDRCorr*. In case the attenuation bias exceeds a configurable barrier, also the respective quality bit is activated in *QZh*. The method is based on the adaptive *PHIDP*- and *ZDR*-constraint approaches described in Bringi and Chandrasekar (2001) and was introduced in Werner and Steinert (2012). The algorithm is performed ray by ray for each clutter-free, connected ray segment of common hydrometeor type, provided by a hydrometeor pre-classification scheme. The latter uses a fuzzy logic approach involving *ZhCorr* and *ZDRCorr* (prior to the attenuation correction), *URHOHV*, and *KDP*, as well as the *zero degree isotherm* and the *snow limit* fields from the *COSMO-DE* NWP model. Since the attenuation correction algorithm hinges on the differential phase, a quality controlled version of this measurement is generated by an iterative smoothing procedure (Hubbert and Bringi (1995)) applied in each of the mentioned ray segments to the data values of *UPHIDP*. The outcome is a revised measurement *PHIDPCorr*. From *PHIDPCorr*, then specific differential phase *KDPCorr* is derived. Note that, as a scheme subsequent to data quality control, the final hydrometeor classification will be performed, then resorting to the attenuation corrected reflectivity *ZhCorr*, differential reflectivity *ZDRCorr*, and *KDPCorr*.

Step 8: *Speckle Filter and Interpolation*
Starting from *UZh* for the reflectivity, from *UZDR* for the differential reflectivity, from *Vh* for the radial velocity, and from *UPHIDP* for the (specific) differential phase, several corrections have been performed in the previous steps, resulting in *ZhCorr*, *ZDRCorr*, *VhCorr*, *PHIDPCorr*, and *KDPCorr*. As a final correction module, speckle filtering and filling of small gaps in the data by interpolation from neighbouring pixels can be performed. For *ZhCorr*, and *KDPCorr* speckle filtering and interpolation is applied. For *ZDRCorr*, and *VhCorr* only speckle filtering takes place. *PHIDPCorr* is not modified.

Step 9: *Bright Band Detection*
Another quality issue marked in the quality product *QZh* is the *bright band*. The detection of this phenomenon is realised as part of the hydrometeor classification performed after the data quality control. It is described in Werner and Steinert (2012).

2.4. Results for an example case

We consider data from the DWD coast radar Rostock (wmo number 10169), on Tuesday, June 10, 2014, 03:55 UTC.

Figure 3 deals with the precipitation scan mentioned in Section 2.1. In the first row on the left, the uncorrected reflectivity *UZh* provided by the signal processor is shown. Although denoted as uncorrected, at least a noise filter was already applied. Echoes from a precipitation event south east of the radar are detected. However, various types of spurious echoes are contained in this data sweep:

- The azimuth sector from 56° to 77° degrees is blanked for safety reasons, because of a building crane located near the radar.
- In the vicinity of the radar, in southern direction, up to about 20 km distance, ground clutter echoes dominate.
- Between 270° and 360°, and between 0° and 45°, ground echoes occur up to the maximum range, due to anomalous propagation of the radar beam.
- Various ship signatures occur, which, in a PPI visualisation, would appear as ring segments. In the present azimuth-range display, these are observed as line structures parallel to the azimuth axis.

The left picture in the fourth row of Figure 3 shows the horizontal reflectivity moment *Zh* provided by the signal processor, which is still used in many applications at DWD. However, many spurious echoes remain. Close to the radar ground clutter remnants are visible, and the ship signatures are still present. Moreover, many of the ground clutter caused by anomalous propagation of the radar beam remains. The right picture in in the first row of Figure 3 shows *ZhCorr* after **Step 2** (application of thresholds) of the scheme described in Section 2.3. The left picture in the second row shows *ZhCorr* after the single-polarisation algorithms in **Step 3**. Many of the ring structures have been partially or completely removed. Right of this plot, the result after the polarimetric clutter detection in **Step 4** is shown. After the attenuation correction, speckle filtering, and interpolation, one ends up with the moment *ZhCorr* depicted in the third row. Only small areas of low reflectivity remain in distances up to 20 km. The ground clutter caused by beam ducting is almost completely removed. Compared to the classical reflectivity *Zh* in the last row, *ZhCorr* represents a much cleaner alternative. The quality product *QZh* (to the right of *Zh*), besides the other quality issues, also shows the detected bright band (**Step 9**). In case more than one quality issue is detected for a single range bin, only the one with the highest precedence according to an arbitrary hierarchy is visible. Note that for many pixels in the vicinity of the radar, the flag *Doppler filter correction valid* is set. This is only done for stationary clutter pixels, which are considered to be adequately treated by the Doppler filter (recall **Step 4**). In this example, however, we have eliminated also these pixels in the final *ZhCorr*. The blanked sector is marked in *QZh* as a negative spoke artifact.

Figure 4 shows *Vh* and *VhCorr* for the $0.5°$ elevation of the volume scan. The considerable impact of the correction of dual-PRF unfolding errors is evident. Especially for the mesocyclone detection scheme, seeking for special patterns of azimuthal shear in radial velocity, this step is vital.

Finally, again for the precipitation scan, in Figure 5, in the first row, original *UZDR*, and the final *ZDRCorr* is depicted. The second row contains *URHOHV* and *UPHIDP*. In the last row, the *KDP* provided by the signal processor, and the one generated by the post-processing quality control are shown.

3. Current and future usage of radar data quality information at DWD

DWD has been operationally using the radar data post-processing quality control tool *RadarQS* since 2009, see Hengstebeck et al. (2010). As the new scheme described above, *RadarQS* generated the quality flag products *QZh*, and *QVh*, except the flags for the assessment of the Doppler filter performance, resorting to single-polarisation measurements. Within DWD, these products are used in data assimilation for the *COSMO-DE* NWP model, cf. Helmert et al. (2012). Moreover, they are used by the hydrology department to generate a quality controlled quantitative precipitation composite. The strategy how the quality flags are applied in these applications clearly differs, being consistent with the idea of flag products. However, initially, these were the only places, where post-processing quality control entered. All other radar products relied on reflectivity *Zh* and radial velocity *Vh* only filtered by means of the signal processor. Now, from the new quality control scheme one may benefit in the following way:

(i) Users may still resort to the quality flag products and design an individual filtering strategy, optionally complemented by the attenuation biases, which can also be separately provided by the new tool. Yet, this requires detailed knowledge of the capabilities of the quality products. Especially, the interpretation and application of the Doppler filter control bits is not easy (recall the non-trivial **Step 4** above).

(ii) Alternatively, subsequent schemes may be directly based on the *ZhCorr* and/or *VhCorr*, and on the other corrected measurements.

Concerning aspect (ii), it is planned to subsequently switch from the usage of *Zh* to *ZhCorr* for the generation of German radar composites and local radar products. Already today, the hydrometeor classification realised in POLARA takes, among other data sources, *ZhCorr*, *ZDRCorr*, and *KDPCorr* as input. The recently developed polarimetric quantitative precipitation estimation (PQPE) algorithm employs *ZhCorr*, and *ZDRCorr*. The latter products are currently being evaluated by DWD's forecasting and hydrologic departments. Once this procedure is completed, it is envisaged to use the PQPE products as a core ingredient in the quantitative precipitation estimation production chain. Finally, already now, the mesocyclone detection algorithm essentially relies on *VhCorr*.

Acknowledgement

I would like to acknowledge the work of my colleagues Dr. Michael Frech, Jörg Steinert, and Dr. Thomas Hengstebeck. Michael Frech is the developer of the radar monitoring tool providing the *Radar Status* files. The hydrometeor pre-classification used in the attenuation correction scheme and for the bright band detection have been developed by Jörg Steinert. The correction of the radial velocity for dual-PRF unfolding errors has been realised by Thomas Hengstebeck.

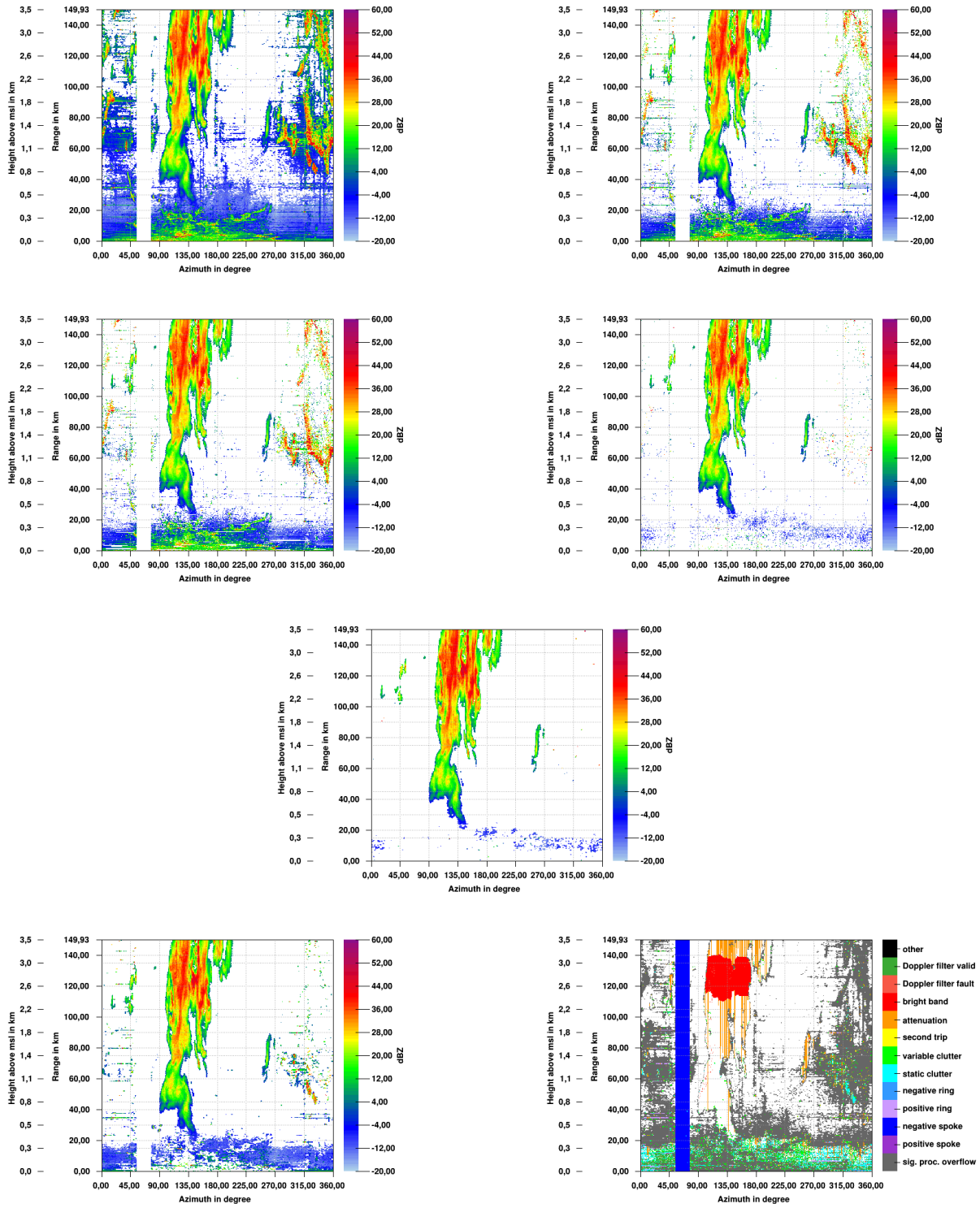

Figure 3: Azimuth-range visualisation of horizontal reflectivity data from DWD radar Rostock, June 10, 2014, 03:55 UTC, precipitation scan mode. Upper row, left to right: *Uncorrected horizontal reflectivity* UZh*, and* ZhCorr *after* ***Step 2***. Second row, left to right: ZhCorr *after* ***Step 3****, and after* ***Step 4***. Third row: *Final* ZhCorr. Last row, left to right: *Horizontal reflectivity* Zh *provided by signal processor, and quality flag product* QZh *corresponding to* Zh.

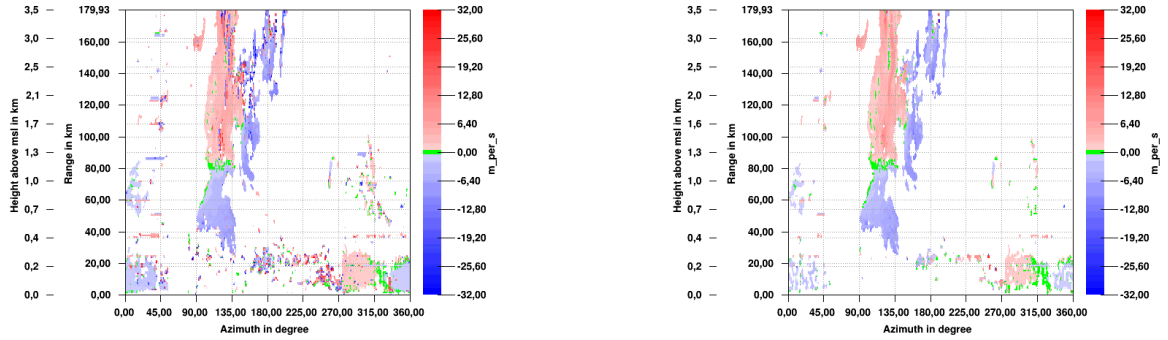

Figure 4: Azimuth-range visualisation of horizontal radial velocity data from DWD radar Rostock, June 10, 2014, 03:55 UTC, volume scan, 0.5°. Left: *Horizontal radial velocity* Vh *produced by signal processor.* Right: VhCorr *produced by post-processing quality control.*

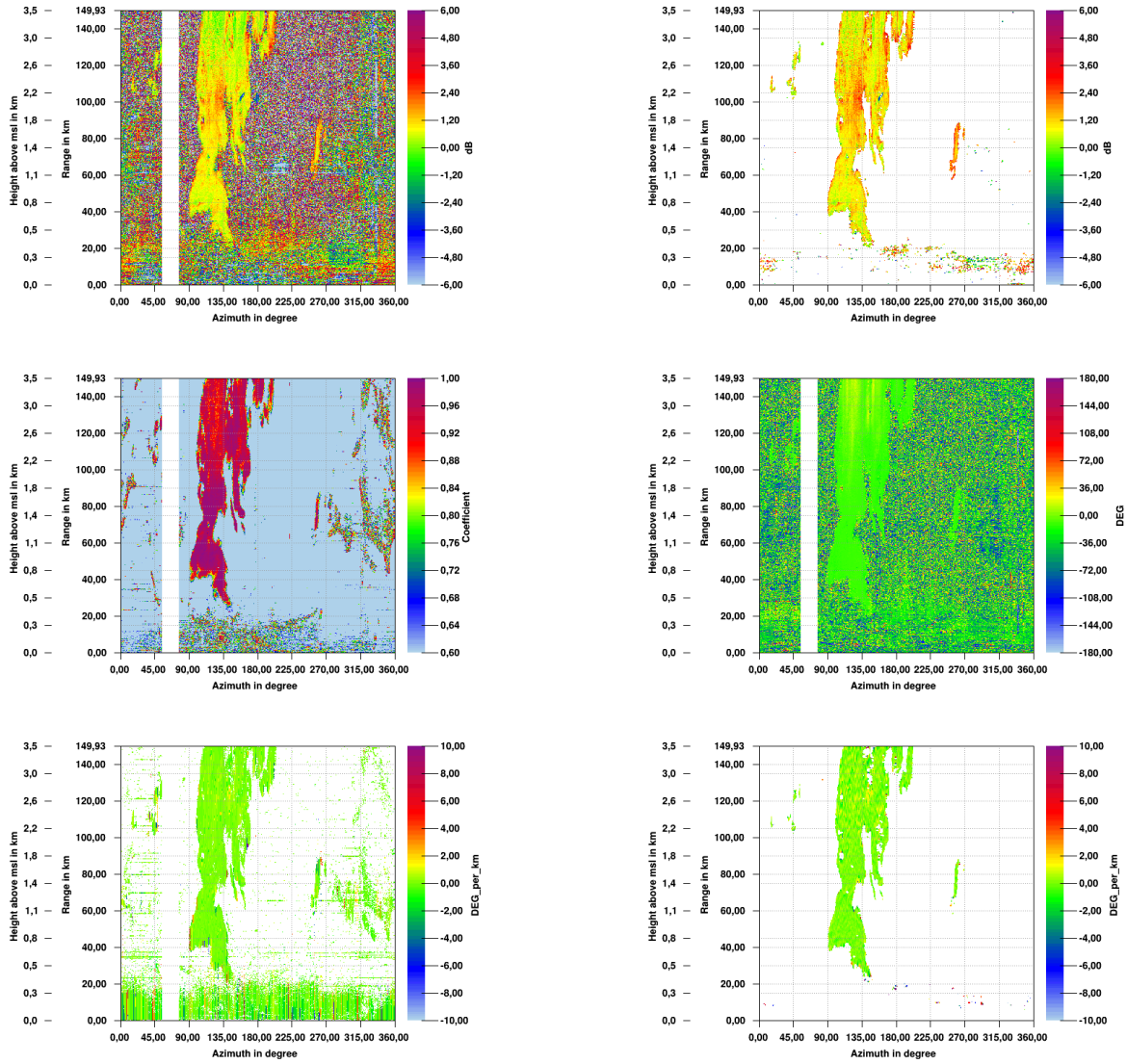

Figure 5: Azimuth-range visualisation of data from DWD radar Rostock, June 10, 2014, 03:55 UTC, precipitation scan mode. First row, left to right: *Uncorrected differential reflectivity* UZDR*, and differential reflectivity* ZDRCorr *generated by post-processing.* Second row, left to right: URHOHV*, and* UPHIDP. Last row, left to right: *Specific differential phase delivered by signal processing, and* KDPCorr *produced by post-processing.*

References

V. Bringi and V. Chandrasekar, *Polarimetric Doppler Weather Radar*. Cambridge University Press, 2001.

M. Frech, "Monitoring the data quality of the new polarimetric weather radar network of the German Meteorological Service," in *36th AMS Conf. on Radar Meteorology*, Breckenridge, CO, USA, 2013.

B. Hassler, K. Helmert, and J. Seltmann, "Identification of spurious precipitation signals in radar data," in *Proc. 4th Europ. Conf. On Radar in Meteor. and Hydrol. ERAD Publication Series 3*, Barcelona, Spain (Göttingen: Copernicus GmbH), September 2006, pp. 590–592.

K. Helmert, T. Hengstebeck, and J. Seltmann, "DWD's operational tool to enhance radar data quality," in *Proc. 5th Europ. Conf. On Radar in Meteor. and Hydrol.*, Helsinki, Finnland, 2008.

K. Helmert, B. Hassler, and J. Seltmann, "An operational tool to quality control 2D radar reflectivity data for assimilation in COSMO-DE," *International Journal of Remote Sensing*, vol. 33, pp. 3456–3471, 2012.

T. Hengstebeck, K. Helmert, and J. Seltmann, "RadarQS - a standard quality control software for radar data at DWD," in *Proc. 6th Europ. Conf. On Radar in Meteor. and Hydrol.*, Sibiu, Romania., 2010.

T. Hengstebeck, D. Heizenreder, P. Joe, and P. Lang, "The mesocyclone detection algorithm of DWD," in *6th European Conference on Severe Storms (ECSS 2011), 3 – 7 October 2011,*, Palma de Mallorca, Balearic Islands, Spain, 2011.

J. Hubbert and V. Bringi, "An iterative filtering technique for the analysis of copolar differential phase and dual-frequency radar measurements," *J. Atmos. Oceanic Technol.*, vol. 12, pp. 643–648, 1995.

N. Rathmann and M. Mott, "Effective radar algorithm software development at the DWD," in *Proc. 7th Europ. Conf. On Radar in Meteor. and Hydrol.*, Toulouse, France, 2012.

T. Schuur, A. Ryzhkov, and P. Heinselman, "Observations and classification of echoes with the polarimetric WSR-88D radar," NOAA/NSSL Report, 45 pp., Tech. Rep., 2003.

J. Steinert, "Hydrometeor classification for the DWD weather radar network: First verification results," in *Proc. 8th Europ. Conf. On Radar in Meteor. and Hydrol.*, Garmisch-Partenkirchen, Germany, 2014.

M. Werner and J. Steinert, "New quality assurance algorithms for the DWD polarimetric C-band weather radar network," in *Proc. 7th Europ. Conf. On Radar in Meteor. and Hydrol.*, Toulouse, France, 2012.